

Signals generated in memristive circuits

Abstract

Signals generated in circuits that include nano-structured elements typically have strongly distinct characteristics, particularly the hysteretic distortion. This is due to memristance, which is one of the key electronic properties of nano-structured materials. In this article, we consider signals generated from a memristive circuit model. We demonstrate numerically that such signals can be efficiently represented in certain custom-designed nonorthogonal bases. The proposed method ensures that the actual numerical representation can be implemented as a fast, $O(N \log N)$, algorithm. In addition, we discuss the possibility of modelling the hysteretic distortion via fast numerical transforms.

Artur Sowa*

*Department of Mathematics and Statistics,
University of Saskatchewan, 106 Wiggins Road, Saskatoon,
SK S7N 5E6, Canada*

Received 30 August 2012

Accepted in revised form 30 October 2012

Keywords

Memristance, nanoelectronics, fast algorithms, nonlinear eigenvalue problems

PACS: 85.35.-p, 02.30.Nw, 02.10.De

MSC: 42C99

© Versita sp. z o.o.

1. Introduction

Several attributes of nanoscale electronics set it apart from its classical predecessor. Among them is the problem of essential variability of nano-patterned circuits, which means that they might need to be assessed and tuned at the essentially individual level. This contrasts with the specifications-based approach to mass fabrication of classical electronics. It is not surprising, therefore, that the variability problem is now recognized as one of the major challenges of next-generation microchip fabrication, [14]. One may expect that a solution of this problem will amount to nothing short of a new paradigm which, compared with the classical approach to microfabrication, will shift even more weight toward the circuit diagnostics, increasing the significance of specialized analytic tools, including mathematical methods for nano-circuit specific signal analysis.

Another distinct attribute of nano-circuits is that they push the scale at which the quantum properties of matter cannot be ignored. The electronic characteristic of structures such as a molecule suspended between metal contacts, [7, 16], or coupled quantum dots or other meta-materials, cannot be understood at the fundamental level outside the framework of Quantum Mechanics. Even though circuits that include nano-patterned elements can to some extent be analyzed by means of a suitably designed classical approach, the classical circuit theory is by itself insufficient. That is in large part due to the emergence of nonlinear and charge-dependent resistance known as the *memristance*.

Nonlinear macro-properties of matter emerge from a quantum linear micro-scale picture through sheer randomness, complexity, and open system dynamics. This can be rigorously considered within the framework of Quantum Statistical Mechanics: nonlinearity enters the quantum-mechanical arena via the von Neumann entropy, which becomes relevant to the functional properties of a non-isolated system through the appropriate free energy. It is interesting to reflect that the nonlinear quantum-mechanical structures possess distinct mathematical flavor that sets them apart from the generally more familiar geometric differential equations. In particular, with some purely-mathematical manipulation of parameters,

* E-mail: sowa@math.usask.ca, a.sowa@mesoscopia.com

these structures may display fairly exotic properties, such as fractal energy spectra, or Riemann's zeta-function related ground states, [22].

Nonlinearity may also enter the arena of quantum- and nano-system modelling via the quantum hydrodynamic models which are often conceptually, as well as computationally, superior to the typically intractable *ab initio* models, [13]. To add to the complexity of the overall picture, nonlinearities may sometimes affect the dynamics of a quantum system via nonlocal integral operators as it happens in the case of the Schrödinger-Poisson models or their extensions, e.g. [12]. Naturally, the list of ways in which nonlinear dynamics becomes relevant to quantum- and nano-systems is much longer and cannot be made complete in this introduction.

A functional macro-scale description of the electronic properties of a given nano-circuit is seldom, if ever, derived directly from the first principles, whether they be linear or nonlinear. A classical approximation of the charge dynamics in a nano-circuit can be based on the aforementioned concept of *memristance*, first proposed theoretically by L. Chua in the 1970s, [4], and experimentally validated in the context of nano-materials only fairly recently, [29]. Memristive materials have since been used in remarkably novel device applications, e.g. in [1] the authors proposed a device based on a layered Au-Pt-TiO_{2-x}-Pt-Ti-SiO₂-Si nano-structure¹ with voltage-pulse-tunable resistive states. They have also indicated an application to analog multiply-and-add computation, which is one of the fundamental operations in information processing. Separately, a joint Hewlett-Packard Laboratories and Boston University project, Cog Ex Machina, focuses on electronic brain models, which rely in an essential way on memristive structures. In this instance, the memristive elements, which amount for no more than 1 percent of the circuitry, enable the essential adaptivity features and memory of the system, [21]. Other applications of memristive circuits, including applications in non-volatile memory or image processing, have been reviewed in [17]. Memristive circuits have also been found to enable energy efficient higher harmonics generation, [6], providing an alternative to the diode bridge which has been traditionally used for this purpose.

It is remarkable that Chua's initial motivation was founded on a rather penetrating insight that the classical RLC circuit theory is mathematically incomplete². The fact that the circuit theory amended with memristance now seems entirely complete builds confidence that this approach is no longer missing anything hidden, and can be used to help predict the implications of more fundamental modelling. It also implies that in essence the functional macroscopic theory of passive nano-circuits is equivalent to the theory of nonlinear, second order ordinary differential equations. This poses mathematical challenges that are typically addressed by means of numerical simulation as well as by means of theoretical analysis that encompasses elements of the Theory of Dynamical Systems. We emphasize that this type of mathematics is indeed fully relevant to nano-circuits, including the rather sophisticated concepts such as chaos, cf. the Chua circuit, [28].

There exist several alternative approaches to the description of complex linear or nonlinear circuits. As observed several decades ago, see [8], [15], one of the mathematical structures naturally emerging in this context is that of the Differential Algebraic Equations (DAE), also referred to as the semi-state equations. An analysis of memristive circuits within the framework of semi-state equations has been carried out in [18]. One of the main theoretical concepts in that work is the *tractability index* arising in the analysis of the DAE.

Among the memristive circuits a special place is occupied by memristor oscillators, cf. [10]. It is therefore interesting to consider the problem of existence of proper oscillations, which leads to differential-algebraic eigenvalue problems (DAEP). The contrast with the classical linear theory is underscored by the fact that such problems typically do not admit closed-form solutions, and are rather difficult to tackle analytically. An approach based on linearization and eigenvalue analysis, as an approximate diagnostic for the existence of proper oscillations, has been explored in [19]. In addition, there exist fruitful fully nonlinear techniques for the analysis of DAEP, which rely on elements of the Analytic Number Theory, [23]. In the framework of this approach a DAEP is set *a priori* in the space of the classical Dirichlet series or, alternatively, in the space of holomorphic Fourier series. This forces discretization of the spectrum. (For comparison, in the classical *linear* Sturm-Liouville theory the latter is accomplished by prescribing the boundary conditions.) The

¹ The memristive properties of such structures may be understood via the linear dopant-drift model, see e.g. [29] or [17]. This model is further refined in [6].

² The nature of this incompleteness is rather subtle but becomes quite ostensible once it is revealed — see Fig. 1 in [29].

method yields an explicit recurrence formula for the series coefficients of the ground state eigenfunction. As it turns out, the higher energy eigenfunctions are dilated versions of the ground state eigenfunction.

The number-theoretic approach to an eigenvalue problem — such as may stem from a nano-circuit of interest — leads to a whole new method of analysis of signals which originate from the circuit. Namely, one first notes that the entire system of eigenfunctions (typically with a modified constant term) can be considered as a basis for a suitable Hilbert space. The basis consists of a ground state function $f(x)$ and its dilated copies $f(mx)$, $m = 1, 2, 3, \dots$. It has been established that such bases have a very unusual property — namely, they furnish fast, $O(N \log N)$, change-of-basis transforms, [24]. In fact, the change of basis can be carried out numerically with extreme efficiency via a lifting schema, [25]. These facts form the precepts of a new method of signal analysis which is numerically efficient and customizable to specific nano-circuits. Moreover, the method presented in [26] allows for a construction of a broad family of fast-transform bases, going beyond the framework of DAEP. Indeed, the paper identifies verifiable sufficient conditions on $f(x)$ for the collection $\{f(mx)\}$, $m = 1, 2, 3, \dots$ to be a Riesz basis. We emphasize that $f(x)$ need not necessarily descend from a DAEP. However, it is demonstrated in [26] that the bases arising from the specific DAEP considered in [24] are in fact Riesz. The Riesz property is of interest from the point of view of applications as it guarantees numerically stable decomposition of a signal in the given basis. However, in practice numerical stability can be established via a numerical experiment.

In this article we describe an application of these new techniques to the analysis of a hypothetical memristive circuit, introduced and numerically simulated in Section 2. As was observed relatively early on, [5], memristive circuits often generate signals with a characteristic hysteretically distorted shape³. In Section 3 we discuss a few topics related to the analysis of hysteretically distorted signals. The main challenge stems from the fact that for the hysteretic features to appear the signal's Fourier series needs to have a significantly long tail. Therefore, an approximation of such a signal by a low degree trigonometric polynomial will erase hysteretic features. (Clearly, this phenomenon may be viewed as a generalized Gibbs effect — see Sections 4–5 for detailed comments.) This becomes a hindrance when one wishes to carry out, say, signal denoising or compression in a way that does not spoil the hysteretic features. Section 3 outlines an approach to this problem, which utilizes a novel fast transform, [24–26]. The discussion culminates in Section 4, where we argue that hysteretic distortion may also be simulated by certain fast transforms.

2. A model for an RLCM circuit

Let us fix four electronic components: a resistor fully characterized by constant resistance R , an inductor with inductance L , a capacitor with capacitance C , and a memristor which is characterized by a charge- and current-dependent memristance $M = M(q, \frac{dq}{dt})$. We consider a circuit that consists of these components connected in a series with an addition of a voltage source $v(t)$. In contrast to the classical RLC circuit it is more convenient to describe the temporal dynamics of an RLCM circuit by charge fluctuations, $q(t)$, rather than the current fluctuations $i = \frac{dq}{dt} = \dot{q}$. In our case $q(t)$ satisfies the equation

$$L \frac{d^2 q}{dt^2} + R \frac{dq}{dt} + M(q, \frac{dq}{dt}) \frac{dq}{dt} + \frac{1}{C} q = v(t). \quad (1)$$

The nonlinear term depends on the particular architecture of the memristor which may be based on a nano-structure, [11]. In order to fix attention henceforth we fix the memristance function as

$$M(q, \frac{dq}{dt}) = M(q) = A \exp(-Bq). \quad (2)$$

Note that Bq needs to be dimensionless, so that the physical unit of B is $[\frac{1}{C}]$, while the unit of A is $[\Omega]$. Our selection of this particular function for M has been motivated by an observation *a posteriori* that it yields a hysteretic distortion of the oscillatory function $t \mapsto q(t)$. This type of distortion is known from experiment to be a characteristic feature of many memristive systems. It should be emphasized, however, that the hysteretic distortion may arise in circuits with other $M = M(q, i)$, e.g. an alternative example is analyzed in [24] and [23].

³ Such distortion is also characteristic for magnetic quantum systems, [20], and for nonlinear electrodynamics, [27].

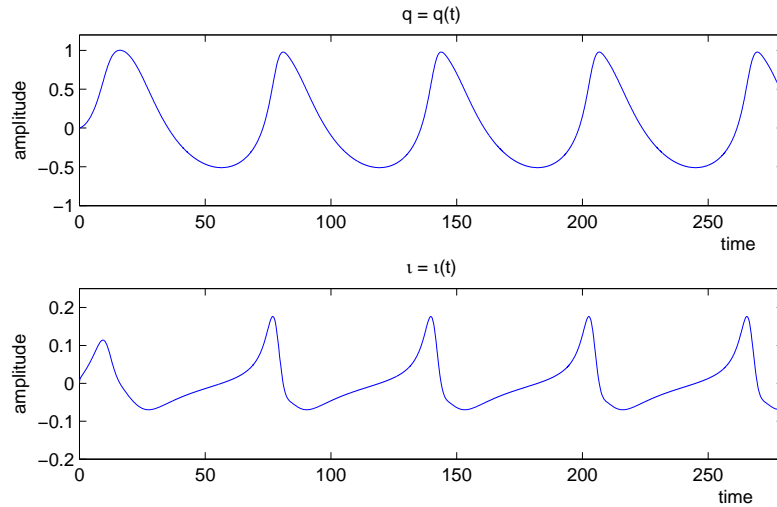


Fig 1. A numerical solution of (3) with $R = L = C = 1$, $\iota(0) = q(0) = 0$, $\omega = .1$, $A = 8$, and $B = 3$. Note that the signal shape during the first cycle is clearly different than in the subsequent cycles. Beginning with the second cycle, $t \mapsto q(t)$ settles in an essentially periodic regime. This indicates that the dynamics has a strong periodic attractor. Note that the oscillatory function $t \mapsto q(t)$ has a sharper slope when it rises than when it falls off. This is the signature of hysteretic distortion. It is often convenient to use the term more loosely, and apply it the type of distortion observed in $t \mapsto \iota(t)$ as well.

Next, we carry out a simulation of the solutions of (1)-(2). For an implementation of an ODE solver, e.g. via the Runge-Kutta method, it is convenient to represent the dynamics in an equivalent *autonomous* form:

$$\begin{cases} \dot{q} = \iota \\ \dot{\iota} = -\frac{1}{LC} q - \frac{R+ Ae^{-Bq}}{L} \iota + \frac{1}{L} \sin u \\ \dot{u} = \omega \end{cases} \quad (3)$$

Note that $\sin u = \sin \omega t$ signifies an oscillatory voltage with amplitude 1. A numerical solution of this dynamical system is displayed in Fig. 1. The reader will observe the hysteretic features of $q(t)$ — namely, the rate of growth of the curve $q(t)$ is faster than the rate of its decay within all the consecutive cycles.

3. Representation of hysteretic signals in special nonorthogonal bases

We wish to consider a few signal analysis problems specifically related to such signals as $q(t)$, or $\iota(t)$ generated in the previous section. First, however, we need to point out a technical point about simulated signals as compared to the natural ones. Namely, signals collected from real systems tend to be given as sampled in regularly spaced time intervals. In contrast, the simulated signals are obtained via a step-adaptive method and so, before any analysis is done, it is necessary to re-sample them in the uniform time-axis grid. However, we have found that for any practical purposes a standard re-sampling method ensures sufficient accuracy. Therefore, from now on we assume that all the signals are prepared in a uniform grid.

Next, we observe that since the signals we work with are real we can take advantage of the *analytic signal method*. Namely, if, say,

$$\iota(t) = \sum_{n \in \mathbb{Z}} y_n \exp(2\pi i n t),$$

then $y_{-n} = \bar{y}_n$. Thus, coefficients with negative indices are redundant and need not be processed. In other words, it is sufficient to analyze the series

$$\iota_h(t) = \sum_{n > 0} y_n \exp(2\pi i n t),$$

and reinsert $y_{-n} = \bar{y}_n$ (and also the constant term y_0) only when the signal needs to be reconstructed, e.g. after a compression and transmission, or after a suitable analysis. We denote the Hilbert space of all square-summable series of this type (non-negative frequencies only) by H_h . (H_h may be referred to it as the space of holomorphic Fourier series).

To simplify our task even further, we extract a single cycle of $u(t)$, denoted $s(t)$ — see Fig. 2. Now, let f denote the holomorphic part of s , i.e.

$$f(t) = s_h(t) = \sum_{n>0} \alpha_n \exp(2\pi i n t), \quad s(t) = f(t) + \bar{f}(t) + \text{const.}$$

We wish to construct a basis of H_h , in which $f(t)$ will have sparse representation. The construction below follows the method established in [24] and [26], and will only be outlined. First, consider the set $\{f(mt)\}$, $m = 1, 2, \dots$, as a candidate for a basis in H_h . Let $\Phi \in H_h$ be an arbitrary vector. It has been demonstrated in [24] that if

$$\Phi(t) = \sum_{m>0} x_m f(mt)$$

then the series coefficients are obtained via

$$(x_1, x_2, \dots)^T = DF\Phi, \tag{4}$$

where F is the Fourier transform, yielding the (positive frequency) Fourier series coefficients, and $D = D(\{\alpha\})$ is the inverse of the infinite matrix determined by the sequence (α_n) as follows⁴:

$$D^{-1} = D^{-1}(\{\alpha\}) = \begin{bmatrix} \alpha_1 & \cdot & \dots \\ \alpha_2 & \alpha_1 & \cdot & \cdot & \cdot & \cdot & \cdot & \cdot & \dots \\ \alpha_3 & \cdot & \alpha_1 & \cdot & \cdot & \cdot & \cdot & \cdot & \dots \\ \alpha_4 & \alpha_2 & \cdot & \alpha_1 & \cdot & \cdot & \cdot & \cdot & \dots \\ \alpha_5 & \cdot & \cdot & \cdot & \alpha_1 & \cdot & \cdot & \cdot & \dots \\ \alpha_6 & \alpha_3 & \alpha_2 & \cdot & \cdot & \alpha_1 & \cdot & \cdot & \dots \\ \alpha_7 & \cdot & \cdot & \cdot & \cdot & \cdot & \alpha_1 & \cdot & \dots \\ \alpha_8 & \alpha_4 & \cdot & \alpha_2 & \cdot & \cdot & \cdot & \alpha_1 & \dots \\ \vdots & \vdots \end{bmatrix} \tag{5}$$

(The dots in the body of the matrix stand in for zeros to help bring out the pattern.) It was observed in [24, 26] that matrices of this type form a ring which is isomorphic to the Dirichlet ring. Article [24] is also devoted to the study of necessary conditions for a set of dilated functions, such as $\{f(mt)\}$, to furnish an unconditional basis. This type of an analytical problem was first addressed in [2]; additional contributions to this theme may also be found in [9].

The unconditionality of the basis typically translates into numerical stability of the corresponding change of basis transform which, for all practical purposes, is easily detected in the course of numerical experimentation. In fact, in the case of $\{f(mt)\}$ defined above, which corresponds to the transform $D(\{\alpha\})F$, we have observed numerical stability.

In the numerical work one only considers truncated vectors and matrices. It was demonstrated in [25] that an evaluation of an N -by- N matrix of type $D(\{\alpha\})$ — that is the upper left corner of the infinite matrix defined above — on a vector of length N can be performed via a lifting schema in $O(N \log N)$ arithmetical operations⁵. Since the well known FFT algorithm performs the discrete Fourier transform in $O(N \log N)$ arithmetical operations, the transform defined in (4) is a fast transform. Note that its inverse is a transform of the same type. A representation of $s(t)$ and $s(2t)$ in the basis constructed in this way is displayed in Fig. 2.

⁴ In practice, in order to ensure numerical stability, it is better to renormalize the sequence α to ensure $\alpha_1 = 1$.
⁵ The exact number of operations is given by the sum-of-divisors function — a few refined estimates of this quantity are discussed in [3] (Ch. VIII).

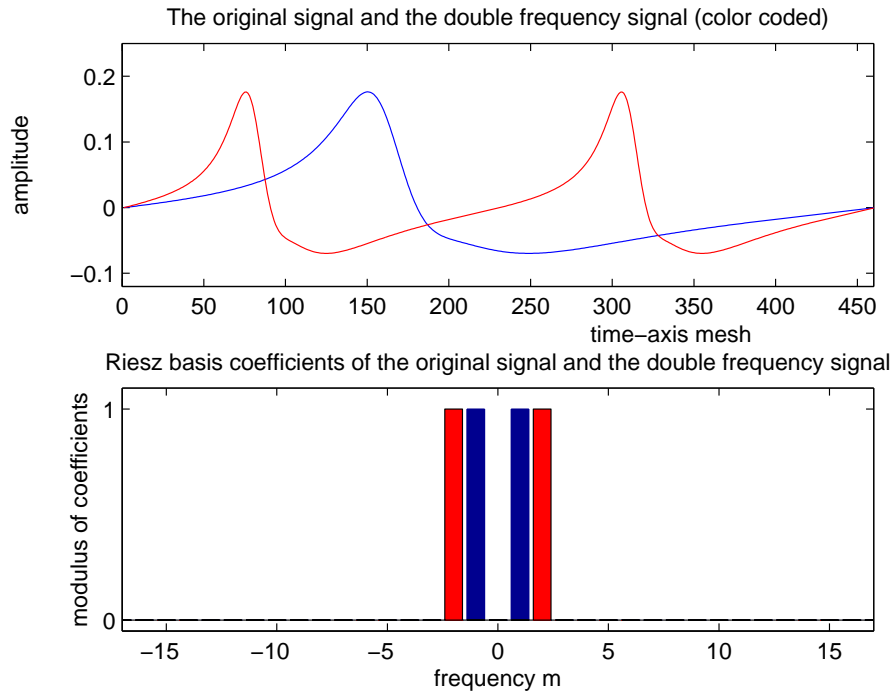


Fig 2. The top graph shows a single-cycle extracted from the signal $s(t)$ denoted in the article text $s(t)$, as well as the double frequency signal $s(2t)$. (For convenience, the horizontal axis is indexed by discretized index points rather than by t .) The bottom figure depicts the coefficients of both signals in the basis $\{\bar{f}(mt)\} \cup \{1\} \cup \{f(mt)\}$ —the outer bars belong to the double frequency signal. Note that the remaining coefficients are in both cases so small as to be imperceptible in this figure. (Note that negative m corresponds to $\bar{f}(mt)$.)

The point of the construction given above is that even when signals are contaminated by noise, as it may happen in the process of measurement, the basis at hand will well separate the deterministic components. This phenomenon is illustrated in Fig. 3. Since the noise energy is evenly distributed over all $f(mt)$ basis vectors, a simple resetting of all small coefficients to zero (*nonlinear thresholding*) results in a reconstruction of the deterministic signal. The reconstructed signal differs from the ideal one by just a small smooth error term. (Depending on the application, the nonlinear thresholding operation may be replaced by a linear low-pass filter.) In Sections 4–5, we shed some light on the nature of hysteretic distortion, and explain why the denoising of hysteretic signals is a hard task to carry out with the Fourier transform alone.

4. Hysteretic distortion via a fast transform

It is interesting to ask if one might use a fast transform to effect hysteretic distortion in a regular oscillatory signal. We provide an affirmative answer by constructing a $O(N \log N)$ transform which effects hysteretic distortion. This is illustrated in Fig. 5, where the input is a simple trigonometric polynomial, and the output is its hysteretically distorted clone.

We begin by considering a “standard” hysteretic wave. Naturally, the physical model of hysteresis which may be based e.g. on ferromagnetism, will result in a somewhat different shape. However, the curve we use captures the essential features of the hysteretic distortion, and has been successfully used in the analysis of quantum magnetic systems, see e.g. [20]. Its main advantage is the mathematical simplicity of the definition. Namely, it is obtained from the transcendental equation

$$x(t) = a \sin[x(t) + t], \quad t \in [0, 2\pi]. \tag{6}$$

Note that the equation can be trivially solved for t , given x . However, we need t to run over a uniform grid, which forces us to solve the equation for x , given t . (An adaptive grid may be desirable in some applications. However, the signal processing algorithms discussed here require a uniform grid.) This can be done with the use of a numerical or

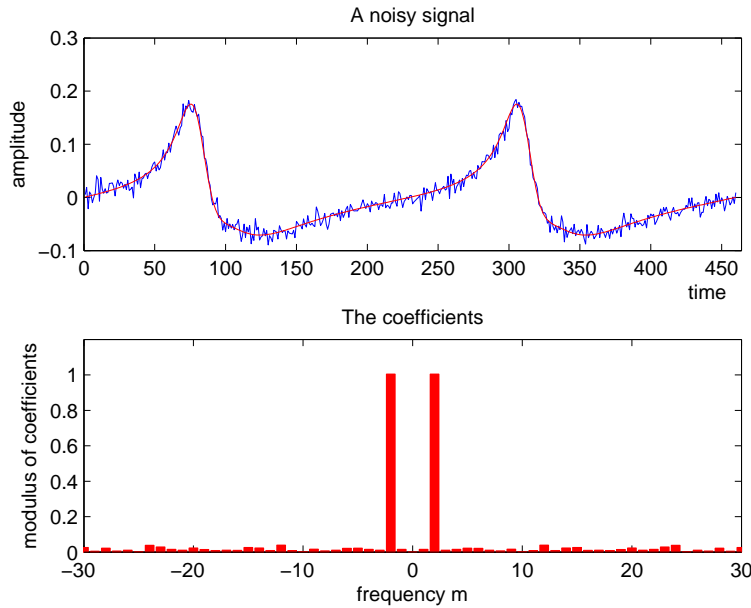


Fig 3. The top graph shows a double frequency signal with additive white noise, and the denoised version (smooth line). The bottom graph shows that almost all the noise is spread evenly through all frequencies in the sense of the $\{f(mt)\}$ basis, which is why a simple nonlinear thresholding (alternatively a low-pass filter) denoises the signal almost perfectly.

symbolic solver. The task is computationally intensive, but trivially parallelizable. Also, the computation needs to be done essentially only once for any grid of interest. Let $x_a(t)$ be the solution corresponding to a given parameter $a > 0$. The parameter controls the strength of the hysteretic distortion as well as the amplitude — examples are displayed in Fig. 4. In general, as a increases the Lipschitz constant characterizing the continuity of the functions $x_a(t)$ increases indefinitely, and past a certain threshold (close to 1), we obtain discontinuous functions. In parallel, the corresponding Fourier series of $x_a(t)$ have increasingly lower diminishing rate for the magnitude of their higher harmonics. Naturally, when a discontinuity appears, which happens for a sufficiently large a , this amounts to the classical Gibbs effect. In this sense, denoising a hysteretically distorted signal by a traditional method of suppressing the high-frequencies will induce Gibbs-type artifacts. While the classical Gibbs artifact is manifested by the introduction of undesirable smoothness near an edge, the weaker version corresponding to hysteretically distorted signals manifests itself via a loss of hysteretic distortion.

Next, let

$$f_a(t) = (x_a)_h(t) = \sum_{n>0} \beta_n \exp(2\pi i n t),$$

and let $\{f_a(mt)\}$ be a basis in H_h . (We do not prove the basis property here.) Finally, let $D_a = D_a(\{\beta\})$ be the corresponding fast transform as defined in (5). We define the following transforms:

$$\Phi \mapsto T_{\text{abs}}[\Phi] := D_a^{-1} |F \Phi|, \quad \Phi \mapsto T_{\mathbb{R}}[\Phi] := D_a^{-1} \Re\{F \Phi\}, \tag{7}$$

where $||$ denotes the pointwise absolute value, and \Re denotes the pointwise real part. Thus $T_{\mathbb{R}}$ is real-linear, while T_{abs} is not linear due to the application of the absolute value. In practice the two transforms have a very similar effect. However, we have observed that in order to ensure a smooth $T_{\mathbb{R}}[\Phi]$ it is necessary to additionally set to zero the small coefficients of $F \Phi$ (either by nonlinear thresholding or by a low pass filter). Note that the pointwise operations, whether linear or not, are carried out in $O(N)$ arithmetical operations. Thus, both transforms have the overall complexity of $O(N \log N)$. The effect of T_{abs} for the signal $\Phi(t) = \sin(2t) + \sin(3t)$ is shown in Fig. 5.

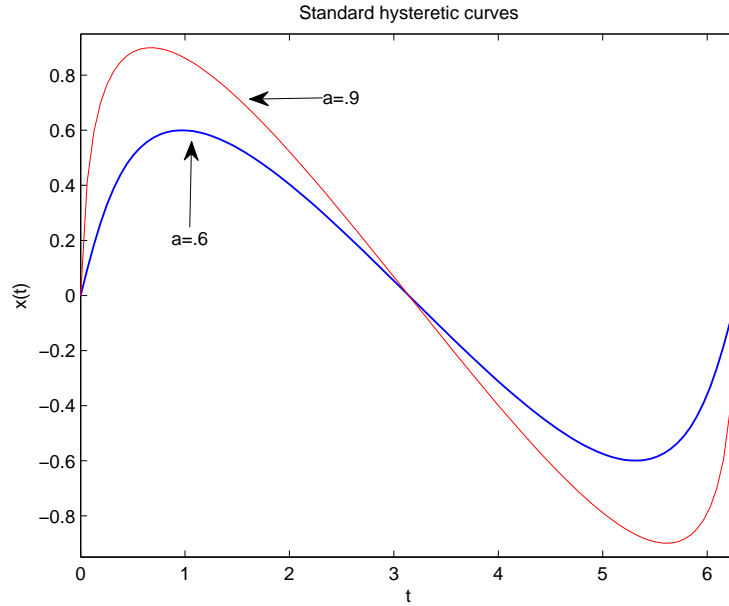


Fig 4. Two solutions $x_a(t)$ of equation (6) over a uniform grid for $t \in [0, 2\pi)$. Note that parameter a controls both the amplitude and the strength of distortion, i.e. how sharply the curve rises and how gently it falls off.

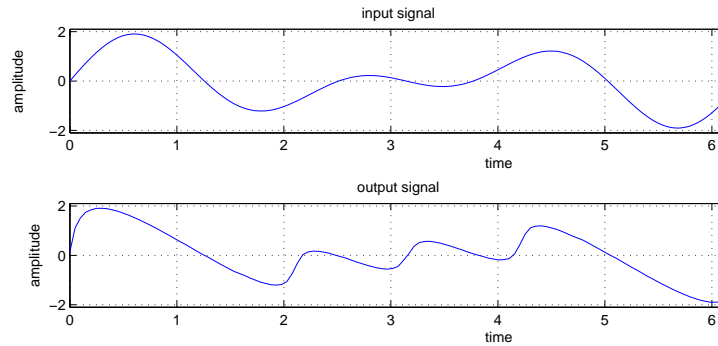


Fig 5. The input is defined as $\phi(t) = \sin(2t) + \sin(3t)$ (top graph), and the output is $T_{\text{abs}}[\phi]$ defined in (7) with $a = .8$.

5. Summary and Closing Remarks

We have seen how memristive circuits can generate oscillatory signals with hysteretic distortion. It has also been outlined how to construct bases of dilated functions which provide sparse representation for hysteretically distorted signals. In addition, we have pointed out that the proposed bases give rise to fast linear transforms, which may typically be expected to display numerical stability.

We have also constructed a fast transform method for inducing hysteretic distortion in an oscillatory signal. Let us point out that the converse task, i.e. removal of hysteretic distortions from a signal, is rather trivial. Indeed, signals with hysteretic distortion possess a long tail of small Fourier coefficients, see Fig. 6. In other words, low-degree trigonometric polynomials do not display hysteretic features. Therefore, a simple approximation by a low degree polynomial will erase the hysteretic feature, and effect a rather significant shape deformation. (As outlined in Section 4 this phenomenon is similar to the classical Gibbs effect.) In comparison, the method proposed in Section 3 shows how to denoise a signal

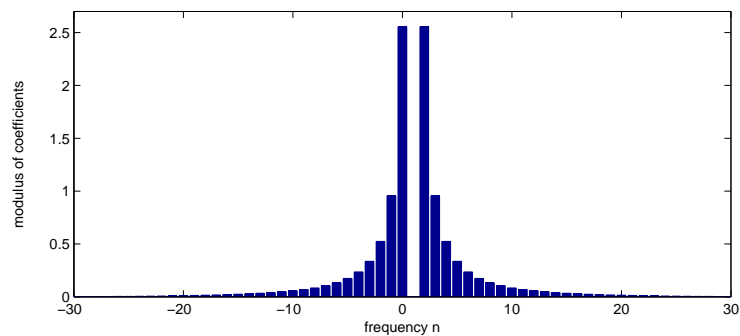


Fig 6. The graph of the Fourier coefficients $\hat{x}_a(n)$ of $x_a(t)$ defined via (6), $a = .9$. Observe the relatively significant spread of significant coefficients.

without any loss of the hysteretic feature. A similar technique is applicable to the task of informational-compression of hysteretically distorted signals.

Acknowledgments

I would like to thank the referees for feedback which led to improvements in the presentation of this material, and especially for bringing to my attention several interesting and relevant references previously unknown to me. I also acknowledge the support of the Canadian Foundation for Innovation, grant LOF 22117.

References

- [1] F. Alibart, L. Gao, B.D. Hoskins, D. B. Strukov. High precision tuning of state for memristive devices by adaptable variation-tolerant algorithm. *Nanotechnology*, **23**, 075201 (7pp) (2012).
- [2] A. Beurling. The Collected Works of Arno Beurling, Vol. 2: Harmonic Analysis, Contemp. Math., Birkhäuser, Boston, 378–380 (1989).
- [3] K. Chandrasekharan. *Arithmetical Functions*, Springer-Verlag, New York, Heidelberg, Berlin (1970).
- [4] L.O. Chua. Memristor - the missing circuit element. *IEEE Trans. Circuit Theory*, **18**, 507–519 (1971).
- [5] L. O. Chua and S. M. Kang. Memristive Devices and Systems. *Proceedings of the IEEE*, **64**, 209–223 (1976).
- [6] G.Z. Cohen, Y.V. Pershin, and M. Di Ventura. Second and higher harmonics generation with memristive circuits. *Appl. Phys. Lett.* **100**, 133109 (2012).
- [7] S. Datta. Nanoscale device modeling: the Green's function method. *Superlattices and Microstructures*, **28**, 253–278 (2000).
- [8] B. Dziurla, R. Newcomb. The Drazin inverse and semi-state equations. In: P. Dewilde (ed.). *Proceedings of the International Symposium on Mathematical Theory of Networks and Systems*. Delft, Netherlands, pp. 283–289 (1979).
- [9] H. Hedenmalm, P. Lindqvist, and K. Seip. A Hilbert Space of Dirichlet Series and Systems of Dilated Functions in $L^2(0, 1)$. *Duke Math. J.*, **86**, 1–37 (1997).
- [10] M. Itoh, L.O. Chua. Memristor oscillators. *International Journal of Bifurcation and Chaos*, **18**, 3183–3206 (2008).
- [11] T.H. Kim, E.Y. Jang, N.J. Lee, D.J. Choi, K.-J. Lee, J.T. Jang, et. al. Nanoparticle Assemblies as Memristors. *Nano Lett.*, **9**, 2229–2233 (2009).
- [12] F. Maucher, S. Skupin and W. Krolikowski. Collapse in the nonlocal nonlinear Schrödinger equation. *Nonlinearity*, **24**, 1987–2001 (2011).
- [13] R.V.N. Melnik, B. Lassen, L.C. Lew Yan Voon, M. Willatzen, C. Galeriu. Accounting for Nonlinearities in Mathematical Modelling of Quantum Dot Structures. *Discrete and Contin. Dyn. Syst.*, suppl., 642–651 (2005).
- [14] M. Miranda. The Threat of Semiconductor Variability. *IEEE Spectrum*, July 2012

- [15] R.W. Newcomb. The semistate description of nonlinear time-variable circuits. *IEEE Transactions on Circuits and Systems*, **28**, 62–71 (1981).
- [16] M. Paulsson, F. Zahid, S. Datta. Resistance of a molecule. In: W.A. Goddard III et al. (editors), *Handbook of Nanoscience, Engineering, and Technology*, CRC Press (2003).
- [17] T. Prodromakis and C. Toumazou. A Review on Memristive Devices and Applications. *IEEE Conference Proceedings: Electronics, Circuits and Systems (ICECS)*, 2010 17th International Conference on, 12–15 Dec 2010, 934–937.
- [18] R. Rianza and C. Tischendorf. Semistate models of electrical circuits including memristors. *Int. J. of Circ. Theor. Appl.*, **39**, 607–627 (2011).
- [19] R. Rianza and C. Tischendorf. Structural characterization of classical and memristive circuits with purely imaginary eigenvalues. *Int. J. of Circ. Theor. Appl.*, (2011). Published online in Wiley Online Library (wileyonlinelibrary.com) DOI: 10.1002/cta.798
- [20] D. Shoenberg. *Magnetic Oscillations in Metals*, Cambridge University Press, Cambridge (1984), (new edition 2009)
- [21] G. Snider, R. Amerson, D. Carter, H. Abdalla, and M. Sh. Qureshi. From Synapses to Circuitry: Using Memristive Memory to Explore the Electronic Brain. *Computer* (Published by the IEEE Computer Society), **44** (2), 21–28 (2011).
- [22] A. Sowa. Spectra of nonlocally bound quantum systems. *Russ. J. Math. Phys.*, **18**, 227–241, (2011).
- [23] A. Sowa. On an eigenvalue problem with a reciprocal-linear term. *Waves in Random and Complex Media*, **22**, 186–206 (2012).
- [24] A. Sowa. A fast-transform basis with hysteretic features. *IEEE Conference Proceedings: Electrical and Computer Engineering (CCECE)*, 2011 24th Canadian Conference on, 8–11 May 2011, 253–257.
- [25] A. Sowa. Factorizing matrices by Dirichlet multiplication. *Lin. Alg. Appl.*, to appear
- [26] A. Sowa. The Dirichlet ring and unconditional bases in $L_2[0, 2\pi]$. (submitted)
- [27] A. Sowa. Magnetic Oscillations and Maxwell Theory. *Phys. Lett. A*, **228**, 347–350 (1997).
- [28] J.C. Sprott. *Elegant Chaos*. World Scientific Publishing Co, London (2010).
- [29] D.B. Strukov, G.S. Snider, D.R. Stewart, and R.S. Williams. The missing memristor found. *Nature Letters*, **453**, 80–83 (2008).